PERFORMANCE OF A COMPACT, CASCADE FCG SYSTEM

J. V. Parker, C. E. Roth
Science Applications International Corporation
2109 Air Park Rd. SE, Albuquerque, NM 87106

S. K. Coffey
NumerEx LLC, 2309 Renard Pl. SE, Albuquerque, NM 87106

F. M. Lehr, J. H. Degnan
Air Force Research Laboratory, Directed Energy Directorate
Kirtland Air Force Base, NM 87117

Abstract

A system of two FCG's coupled via "flux-trapping" is described. The driver FCG, designated SAM, was custom-designed for this application. The output of SAM is a single-turn loop that is tightly coupled to the first winding section of a larger FCG, designated JILL. The single-turn driver loop, coupled to 35 turns of the input winding of JILL, provides a calculated flux gain of 28.

For the first experimental test of the SAM/JILL system, the SAM generator was seeded with 1.0 kA (flux 0.29 Wb) and produced a current of 472 kA (flux 0.10 Wb) in the coupling loop at crowbar time of the JILL generator. Based on the calculated mutual inductance of 5.95 μH, the JILL generator began operation with a seed flux of 2.81 Wb. With this seed flux, the expected output current for JILL driving a 0.8 μH load is 1.8 MA. The measured output current was 884 kA, roughly one half of the expected current. Analysis of the I-dot data from the test shows that this low performance was due to multiple electrical breakdowns in the JILL generator during the interval when the armature-stator contact point was underneath the coupling loop.

Subsequent analysis suggests that the electrical breakdowns were the result of flux compression in the coupling loop. Details of the experiment and analysis will be presented. A modification to the SAM/JILL apparatus is proposed to eliminate electrical breakdown.

I. INTRODUCTION

The very high energy and energy-density available from explosive pulsed power (EPP) devices make them a logical choice for applications requiring portability. Portability, however, often requires that the initial energy source used to seed the EPP device also be small, leading to a requirement for large energy gain in the system. For example, a shoe-box sized seed source may provide 100 J of energy to an EPP device providing an output of 10 MJ, an energy gain of 10^5. It is difficult to achieve such a high gain in a single EPP device because flux loss becomes prohibitive.

A solution to this dilemma was demonstrated several decades ago [1], as illustrated in Fig. 1. A cascade of two or more helical flux compression generators are coupled together by inter-stage transformers. The transformers are able to multiply flux, making up for the loss of flux in each stage and, in many cases, increasing the total flux in subsequent stages. As one can see from Fig. 1, however, the transformer approach does have some drawbacks with regard to portability.

Figure 1. Transformer-coupled cascade generators [1]

A much more compact form of transformer coupling is the so-call "flux-trapping" design [2] shown is Fig. 2. In this design several helical FCG's share a common armature. The output of each stage is coupled inductively to the beginning of the next stage stator winding. The stator winding of the next stage is an open circuit until the coupled flux reaches its peak. The flux is then "trapped" when the expanding armature contacts the stator winding.

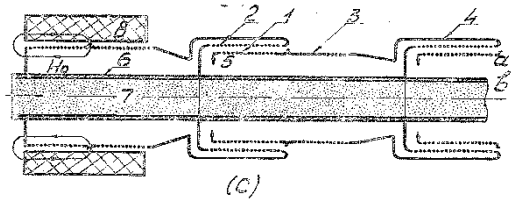

Figure 2. Transformer-coupling by "flux trapping" [2]

Several small generators have been built using this "flux trapping" approach, but their performance has been limited by the difficulty of achieving good coupling in this compact geometry.

The compact, cascade FCG presented in this paper is a hybrid of these two approaches. It employs a separate helical FCG for each stage, allowing optimization of the individual generator designs. Coupling between stages employs the "flux trapping" technique where the output of the first stage is directly coupled to the stator windings of the second stage. Figure 3 shows the combined generators on the firing pad prior to testing.

Report Documentation Page

Form Approved
OMB No. 0704-0188

1. REPORT DATE	2. REPORT TYPE	3. DATES COVERED
JUN 2009	**N/A**	**-**

4. TITLE AND SUBTITLE	5a. CONTRACT NUMBER
Performance Of A Compact, Cascade Fcg System	5b. GRANT NUMBER
	5c. PROGRAM ELEMENT NUMBER
6. AUTHOR(S)	5d. PROJECT NUMBER
	5e. TASK NUMBER
	5f. WORK UNIT NUMBER
7. PERFORMING ORGANIZATION NAME(S) AND ADDRESS(ES) **Science Applications International Corporation 2109 Air Park Rd. SE, Albuquerque, NM 87106**	8. PERFORMING ORGANIZATION REPORT NUMBER
9. SPONSORING/MONITORING AGENCY NAME(S) AND ADDRESS(ES)	10. SPONSOR/MONITOR'S ACRONYM(S)
	11. SPONSOR/MONITOR'S REPORT NUMBER(S)

12. DISTRIBUTION/AVAILABILITY STATEMENT

Approved for public release, distribution unlimited

13. SUPPLEMENTARY NOTES

See also ADM002371. 2013 IEEE Pulsed Power Conference, Digest of Technical Papers 1976-2013, and Abstracts of the 2013 IEEE International Conference on Plasma Science. IEEE International Pulsed Power Conference (19th). Held in San Francisco, CA on 16-21 June 2013., The original document contains color images.

14. ABSTRACT

A system of two FCGs coupled via flux-trapping is described. The driver FCG, designated SAM, was custom-designed for this application. The output of SAM is a single-turn loop that is tightly coupled to the first winding section of a larger FCG, designated JILL. The single-turn driver loop, coupled to 35 turns of the input winding of JILL, provides a calculated flux gain of 28. For the first experimental test of the SAM/JILL system, the SAM generator was seeded with 1.0 kA (flux 0.29 Wb) and produced a current of 472 kA (flux 0.10 Wb) in the coupling loop at crowbar time of the JILL generator. Based on the calculated mutual inductance of 5.95 H, the JILL generator began operation with a seed flux of 2.81 Wb. With this seed flux, the expected output current for JILL driving a 0.8 H load is 1.8 MA. The measured output current was 884 kA, roughly one half of the expected current. Analysis of the I-dot data from the test shows that this low performance was due to multiple electrical breakdowns in the JILL generator during the interval when the armature-stator contact point was underneath the coupling loop. Subsequent analysis suggests that the electrical breakdowns were the result of flux compression in the coupling loop. Details of the experiment and analysis will be presented. A modification to the SAM/JILL apparatus is proposed to eliminate electrical breakdown.

15. SUBJECT TERMS

16. SECURITY CLASSIFICATION OF:			17. LIMITATION OF ABSTRACT	18. NUMBER OF PAGES	19a. NAME OF RESPONSIBLE PERSON
a. REPORT **unclassified**	b. ABSTRACT **unclassified**	c. THIS PAGE **unclassified**	**SAR**	**6**	

Standard Form 298 (Rev. 8-98)
Prescribed by ANSI Std Z39-18

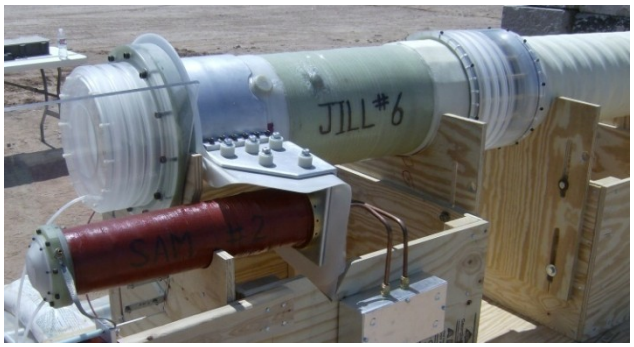

Figure 3. Compact, cascade generator

The small generator in the foreground, designated SAM, is the first stage. The output of SAM is coupled through a parallel-plate transmission line to a single turn loop wrapped around the stator winding of the second stage. The second stage generator, designated JILL, has been described previously as a stand-alone device [3].

The design and testing of the SAM generator are discussed in Sections II and III. Testing of the combined SAM/JILL device is the subject of Section IV, followed by an analysis of the experimental results and proposed design improvements is Sections V and VI.

II. DESIGN OF THE SAM FCG

Design of the SAM generator began with calculations of the coupling loop inductance and its mutual inductance to the JILL generator. Figure 4 shows a cross-section drawing of the coupling loop geometry relative to the stator windings of the JILL generator.

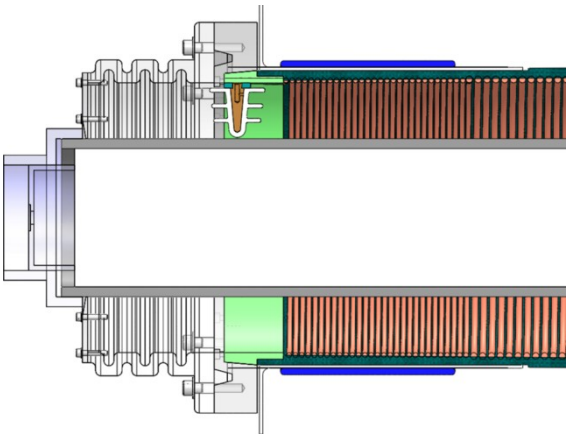
Figure 4. Geometry of the coupling loop (blue) relative to the stator windings of JILL.

The coupling loop is as closely coupled to the stator winding as is practical, given the insulation required to isolate the loop from the high voltage induced in the stator winding. The length of the coupling loop was chosen to be approximately as long as the first section of the JILL stator. This winding section comprises 29 turns of # 6 AWG wire. There is also some coupling to the second stator section which has 17 turns of #4 AWG wire. After optimizing the axial position of the coupling loop, the calculated mutual inductance is 5.57 μH and the self-inductance of the loop, including the effect of the armature, is 208 nH.

The JILL generator has an initial inductance of 314 mH and an initial flux requirement of 3.45 Wb at a typical input current of 11 kA. In order to provide an equivalent input flux, the SAM generator must deliver a current of 619 kA to the coupling loop and a flux of 0.128 Wb. The flux multiplication achieved by transformer action is 26.8 indicating good coupling to the 29+ turns of the JILL stator. The energy coupling efficiency is not particularly good, however. The coupling coefficient between loop and generator, given by the mutual inductance divided by the square root of loop inductance times generator inductance, is 0.69. This rather low value is not surprising considering that the loop does not couple to a substantial fraction of the JILL stator windings. Less than half of the SAM output energy ($0.69^2 = 0.475$) is coupled into JILL, but this seems an acceptable compromise to achieve a large flux gain.

A small, self-contained power supply was available to provide up to 500 J of initial energy for SAM. The final design details for SAM, shown in Table 1, followed directly from the specified input and output requirements. The stator is wound in eight sections. The first five sections provide an approximately logarithmic inductance gradient to maintain constant internal voltage. The last three winding sections are tailored to generate nearly constant I-dot.

Table 1. Design specifications for the SAM generator

Stator Dia.	100 mm	Stator Length	493 mm
Armature Dia.	60 mm		
Inductance	303 μH	Load Induct.	208 nH
Internal Voltage	<55 kV	Peak I-dot	22 kA/μs
Input Current	1.31 kA	Output Cur.	619 kA
Input Energy	260 J	Output Energy	40 kJ
Input Flux	0.4 Wb	Output Flux	0.13 Wb

This is not the usual mode of operation for a helical FCG but was necessary for SAM to avoid inducing excessive voltage in the JILL stator winding. The design goal was to maintain I-dot < 2.2×10^{10} A/s which corresponds to an induced voltage of 122 kV. This was considered to be a safe value since JILL has been operated with internal voltage as high as 140 kV.Figure 5 shows a cutaway drawing of the SAM generator. The design is generally conservative since the physical size had little impact on the overall size of the system. The only unconventional aspect of this design is the radial output connection which was adopted to facilitate interfacing with the flat-plate transmission line.

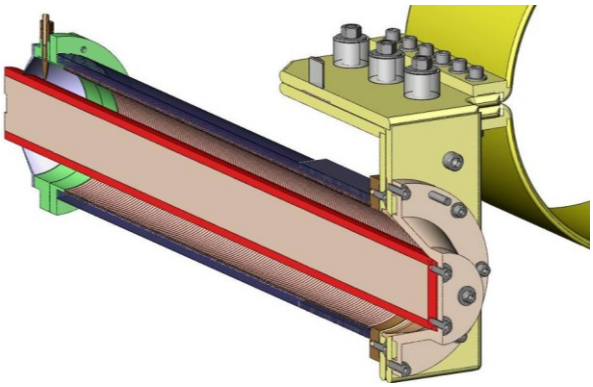

Figure 5. Cross-section drawing of the SAM generator and its connection to the coupling loop.

III. SAM GENERATOR TESTING

The SAM generator was tested with a static load to verify the design. The test setup, Figure 6, shows the coupling loop with a section of 6" (15.2 cm) diameter aluminum pipe simulating the JILL armature. The seed current for this test was 1.17 kA, yielding a peak output current of 488 kA. This corresponds to an average flux transport coefficient of 0.835, somewhat lower than the design assumption of 0.85.

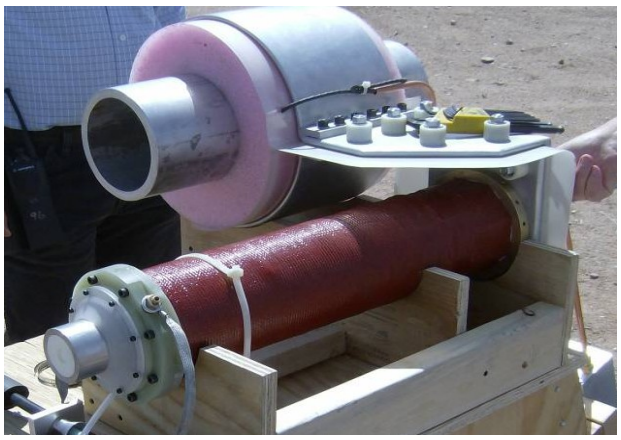

Figure 6. Test setup for initial performance evaluation of the SAM generator.

A plot of I-dot for this test is shown in Figure 7. The three I-dot peaks preceding the end of operation correspond to the last three winding sections of the stator. The intent of achieving constant I-dot in these last three winding sections has been achieved, with only 16% variation in peak I-dot among the three sections.

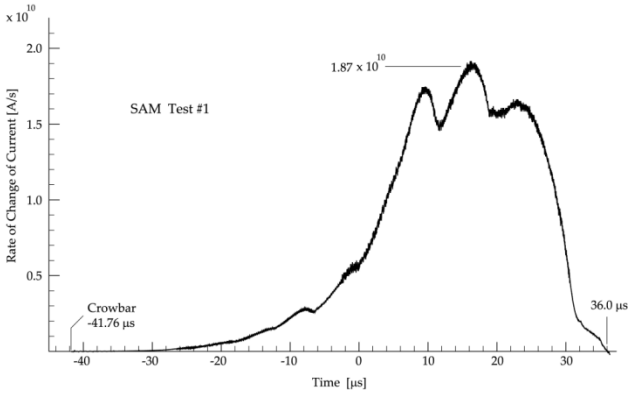

Figure 7. Measured dI/dt for SAM driving a static load.

The overall performance, relative to the calculated design, can be seen in Figure 8 where I-dot/I is plotted and compared to the calculated ideal performance, L-dot/L. Flux loss is nearly uniform throughout generator operation and there is no evidence of electrical breakdowns.

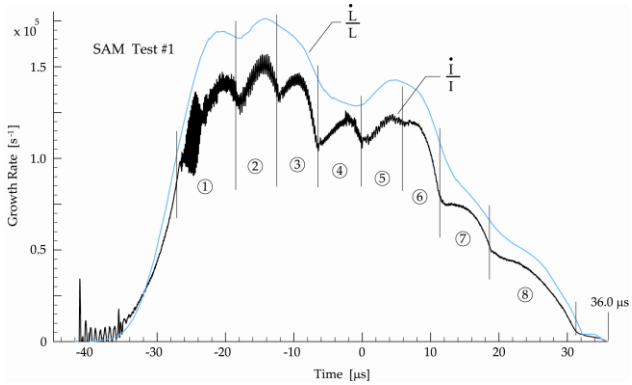

Figure 8. Plot of I-dot/I for SAM compared to the ideal performance, L-dot/L. Position of the eight winding sections is shown for reference.

IV. SAM/JILL TESTING

Following the successful test of a SAM generator, apparatus was assembled for a full SAM/JILL test. The JILL generator, #6 of the series, differs from the standard JILL design in a few details. There is an extra polyethylene insulator between JILL and the coupling loop. The cable input lead is eliminated and extra insulation is added to the crowbar pin to prevent a premature breakdown at the 100+ kV induced voltage. The SAM/JILL system being set up for test was shown earlier in Fig. 3.

The first SAM/JILL test was conducted at a reduced input current of 1.0 kA. The SAM generator performed as designed, producing a peak output current of 472 kA. This was about 5% higher than expected based on the previous SAM test. The average flux transport coefficient was 0.845, closer to the original design estimate of 0.85.

The 472 kA output current translates to a delivered flux of 2.63 Wb in the JILL generator. With this starting flux, the predicted output current from JILL into a 0.8 µH load

is 1.67 MA. The measured current was 0.88 MA, just over one half of the predicted value.

Our usual procedure for examining generator operation, plotting I-dot/I for comparison with L-dot/L, does not work properly for a flux trapping generator because the usual seed current has been replaced by a seed magnetic flux. This results in I=0 at the beginning of operation ans an infinite value for I-dot/I. However, I-dot/I is useful after the armature contact has passed beyond the coupling loop because the seed flux has been converted to generator current at that point. This is evident in Figure 9 which shows I-dot/I for the SAM/JILL experiment.

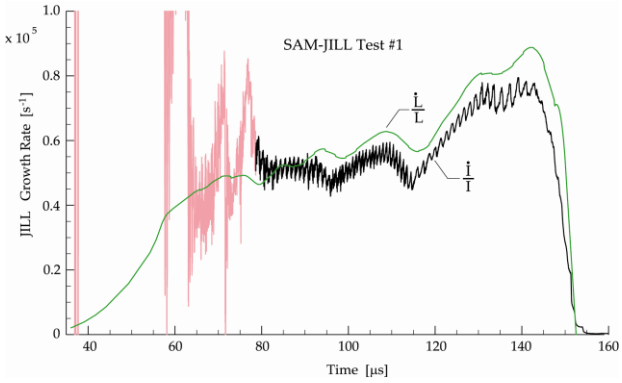

Figure 9. Plot of I-dot/I for SAM/JILL test #1. The plot is off-scale at early time because the current starts at zero..

The black portion of the trace for t > 80 μs corresponds to operation after the armature/stator contact has moved out from under the coupling loop. During this interval the JILL generator appears to be operating normally.

One can obtain a qualitative picture of generator operation at early time by assuming that there is an initial seed current given by the seed flux divided by the JILL inductance, in this case 8.38 kA. This plot, shown in Figure 10, clearly shows that the poor performance was caused by three severe electrical breakdowns that occurred while the armature/stator contact was under the coupling loop.

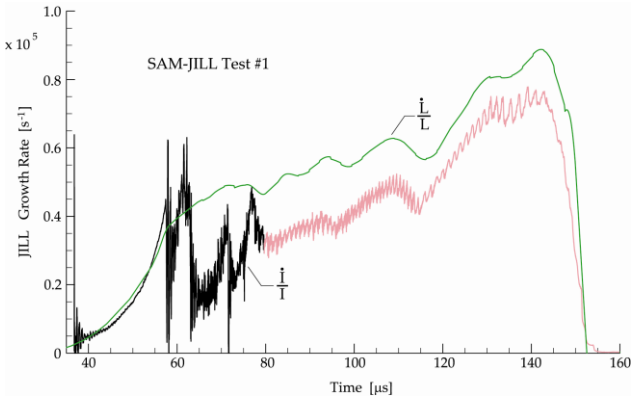

Figure 10. Re-plot of I-dot/I for SAM/JILL test #1 assuming a seed current of 8.38 kA to approximate the initial flux injected by SAM.

In an attempt to understand the cause of these electrical breakdowns, a detailed model of the flux-trapping system was developed using calculated values for the time-dependent self and mutual inductance of the coupling loop. This model predicted that the current in the coupling loop was amplified by flux compression to over 1 MA, assuming that the loop circuit remained intact. This seems likely based on framing camera images of the experiment showing very little motion of the coupling loop during the relevant time. The effect of this amplified loop current on generator operation is examined in the next Section.

V. ANALYSIS

This analysis is focused on the magnetic field configuration in the JILL generator and its implications concerning the internal voltage. For comparison with subsequent calculations, Figure 11 shows the calculated magnetic field lines for a conventional JILL generator at the point in time corresponding to the second electrical breakdown seen in Fig. 9.

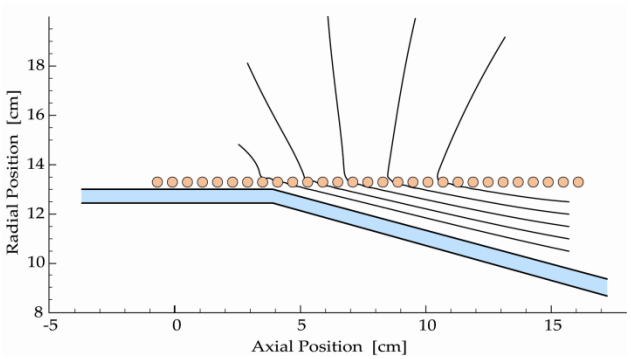

Figure 11. Calculated magnetic field in a conventional JILL generator.

The magnetic field lines are exiting through the stator windings relatively uniformly through 12 to 15 winding turns. Since it is these exiting field lines that generate voltage in the stator winding, this configuration corresponds to a gradual increase in voltage from turn to turn.

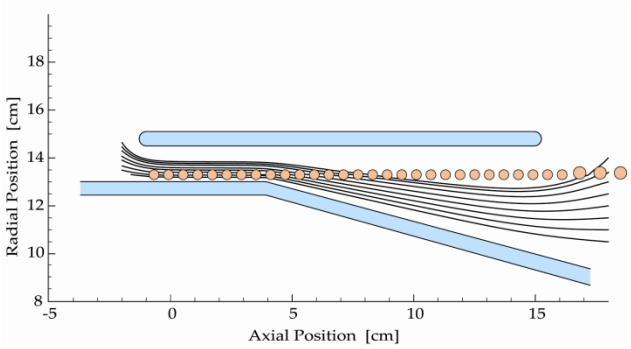

Figure 12. Calculated magnetic field in the JILL generator with a coupling loop carrying 900 kA.

Figure 12 shows the same calculation but now the coupling loop is in place. The loop current, which was

472 kA originally, has been increased by flux compression to 900 kA.

The combination of the enhanced magnetic field from the loop and the proximity of the armature has forced all of the field generated by the JILL stator current to exit the stator winding in a region encompassing only 2 or 3 turns of the winding. The field generated by the amplified loop current cannot generate any net voltage in the stator winding. However, it is apparent from the field line geometry that the loop field is generating an increased voltage under the coupling loop, a voltage that is cancelled out when the same field lines enter through the stator winding to the right of the loop.

In light of this calculation, it is not surprising that strong breakdowns occurred during SAM/JILL test #1. Not only is the generated voltage higher, but it reaches its peak much closer to the armature/stator contact point resulting in an internal electric field that is two to three times higher than the field in a conventional JILL generator.

Although the proximity of the coupling to the stator winding plays a role in creating electrical breakdowns, it is the high current in the coupling loop that is the critical factor. Figure 13 presents the results of the same calculation shown in Fig. 12, but with the loop current set to zero.

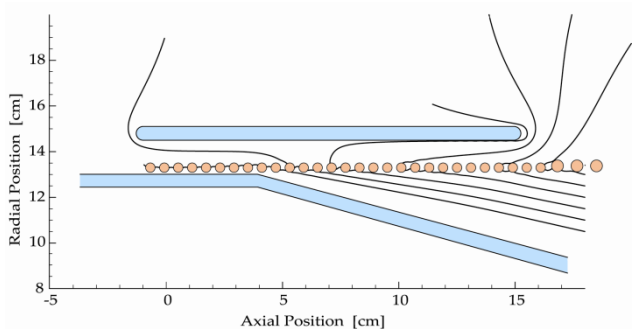

Figure 13. Results of the same calculation shown in Fig. 12, but with the coupling loop current = 0.

Despite the proximity of the coupling loop, the internal magnetic field and its interaction with the stator windings is essentially identical to the conventional JILL result shown in Fig. 11. Thus, there is every expectation that the SAM/JILL compact design will work as designed if the loop current can be reduced or eliminated.

VI. REVISED DESIGN

The coupling loop current must be at its design value when the JILL generator crowbars to provide the required seed flux. Approximately 30 μs later, when the armature/stator contact point passes under the coupling loop, the loop current needs to be as close to zero as possible.

This does not appear to be a particularly challenging task. The majority of the current in the coupling loop was generated by SAM in a time of 25 μs. An aluminum foil fuse, properly designed and mounted, can generally quench the current in an inductive circuit in a time equal to 1/5 of the time taken to establish the current. In this case that time is ~ 5 μs, substantially less than the 30 μs available.

The effect of a fuse in the coupling loop circuit was investigated by adding an aluminum fuse model to the coupled circuit model of the SAM/JILL system. Figure 14 shows the predicted coupling loop current with and without the fuse. The fuse for this calculation had an area of 12 mm^2 and a length of 60 mm. Without the fuse, the calculated loop current is 820 kA when the armature/stator contact point reaches the loop and greater than 1.5 MA when it reaches the end of the loop.

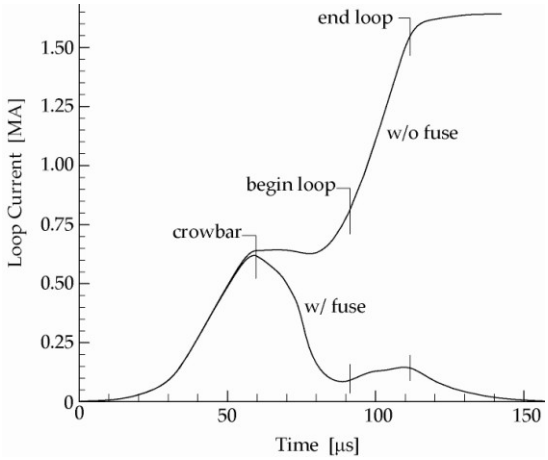

Figure 14. Calculated effect of an aluminum fuse on the coupling loop current.

Adding a fuse to the circuit has a dramatic effect on the loop current. During the interval when the armature/stator contact is passing under the coupling loop the current ranges from 90 kA to 125 kA. Although the current has not been reduced to zero, it is low enough that the internal voltage should be below the demonstrated 140 kV capability of the JILL generator.

The cross-sectional area of the fuse element must be carefully chosen so that the loop current is not reduced prior to JILL crowbar. In the calculation shown in Fig. 14, the current at crowbar has been reduced about 20 kA, from 639 kA to 619 kA. One of the drawbacks to a passive fuse is sensitivity to initial seed current. Once a fuse has been installed, the applied seed current should be maintained within rough 10% of the design value to obtain proper fuse action.

A second SAM/JILL system has been built to investigate whether a fuse will eliminate internal breakdowns. Figure 15 shows the assembled apparatus. The fuse is attached to the coupling loop on the side opposite the SAM generator using the same parallel-plate transmission line hardware. The fuse element is made from 0.10 mm aluminum foil and it is surrounded by fine sand to assist in quenching fuse conduction after burst.

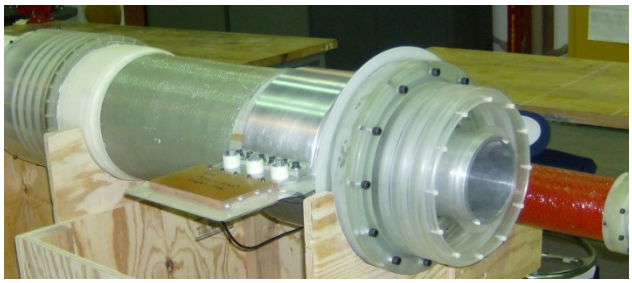

Figure 15. Apparatus for SAM/JILL test #2. The aluminum foil fuse to quench loop current is located in the brown phenolic box projecting out from the loop.

VII. REFERENCES

[1] A. I Pavlovski, et. al., "A Multi-wire, Helical Magnetic Cumulation Generator," in Proc. International Conference on Megagauss Magnetic Field Generation and Related Topics, 1979, pp 585-593.

[2] A. I. Pavlovski, et. al.,"Magnetic Cumulation Generator Parameters and Means to Improve Them," in Proc. International Conference on Megagauss Magnetic Field Generation and Related Topics, 1979, pp 557-583.

[3] J. V. Parker, et. al., "Development and testing of a High-Gain Magnetic Flux Compression Generator," in Proc. of the 2006 International Conference on Megagauss Magnetic Field Generation and Related Topics, 2006, pp. 265-274.